An Application of REE-in-Two-Pyroxene Thermometry to H Chondrites: Evidence for Early Fragmentation—Reassembly of the H Chondrite Parent Body

Michael P. Lucas[1], Nick Dygert[1], Allan D. Patchen[1], Nathaniel R. Miller[2], and Harry Y. McSween[1], [1]Department of Earth & Planetary Sciences, University of Tennessee, Knoxville (mlucas9@vols.utk.edu), [2]Department of Geological Sciences, University of Texas at Austin.

Introduction: Thermal evolution models of asteroids are ground-truthed by estimates of temperatures (hereafter temps) and cooling rates from meteorite cosmochemical data [e.g., 1]. However, traditional geothermometers used to constrain the thermal evolution of meteorite parent bodies typically record blocking temps during cooling rather than peak or magmatic temps. Recently, a REE-in-two pyroxene thermometer was developed [2] that relies on the relatively slow diffusive exchange of REEs between coexisting pyroxenes. This method has been shown to record near-peak or magmatic temps for samples from a variety of geologic settings in the Earth's mantle and crust, and some samples from planetary environments [2-5]. Here, we apply the REE-in-two pyroxene thermometer to six H ordinary chondrites to provide key near-peak temp data. These data, accompanied by major element geothermometry, furnish new insights into the thermal histories of H chondrites. Accurate thermal histories in turn help to discriminate between competing models regarding the geologic evolution of the H chondrite parent body.

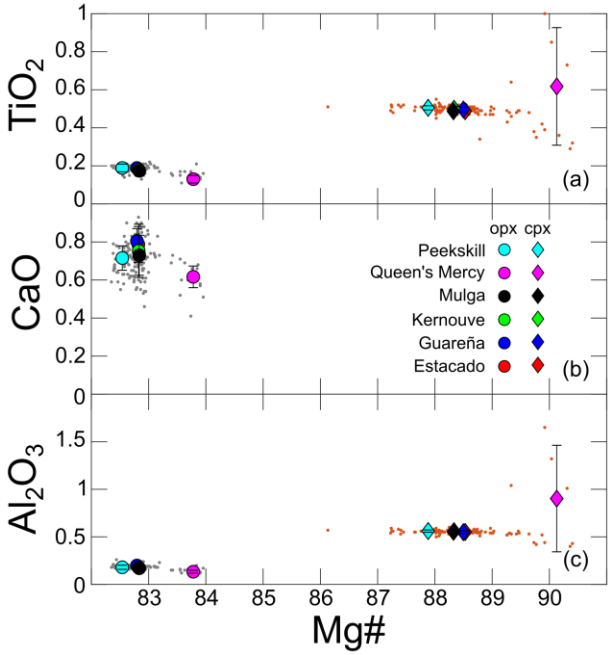

Figure 1. Major element variations in six H chondrites. Small gray (opx) and orange (cpx) dots show the range of mineral compositions among all samples; large circles and diamonds are averaged compositions of grains analyzed by LA-ICP-MS.

Samples and Methods: We selected six H chondrites of high metamorphic grade (H6) for analysis (see Table). Existing temp and cooling rate data for Estacado, Guareña, and Kernouve are compiled in [6,7] and provide a useful benchmark for comparison. Polished thin and thick sections were provided by the Smithsonian NMNH. Orthopyroxene (opx), clinopyroxene (cpx), and olivine (ol) were identified using X-ray maps and analyzed via EPMA at the University of Tennessee with a focused 30 nA, 15 kV beam. For Ca-in-ol, we used a count time of 150 s to achieve a detection limit for CaO=0.011 wt%. Selected REEs, Y, Ti, Sc, and Zr were measured in opx and cpx by LA-ICP-MS at the University of Texas with a laser fluence of ~7.8 J/cm^2 at 8 Hz. We focused on the largest inclusion-free grain pairs we could identify, particularly pairs in close proximity to each other to maximize the potential for chemical equilibrium. We typically used laser spot sizes of 50-75 µm; detection limits for REEs at these analytical conditions are ~20-60 ppb.

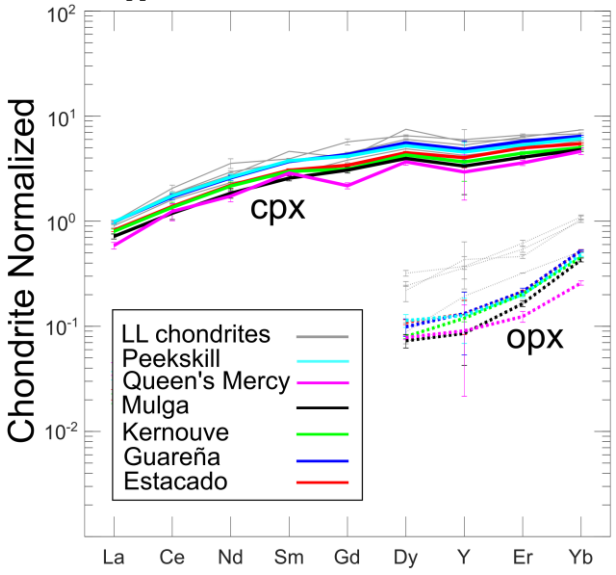

Figure 2. Chondrite normalized REE+Y abundances in cpx (solid lines) and opx (dotted lines). Error bars are 1σ standard deviations of replicate analyses. Shown for comparison are the range of values in four LL chondrites [8] (light gray lines).

Major and Trace Elements: Major elements are plotted in Fig. 1. Clouds of gray (opx) and orange (cpx) dots show averaged compositions of all grains analyzed (opx *n*=146; cpx *n*=124). Averaged compositions of grains analyzed by LA-ICP-MS are plotted using large symbols. Error bars indicate 1σ standard deviations and generally demonstrate compositional homogeneity. Chondrite normalized REE+Y abundances are shown in Fig. 2. Replicate analyses of multiple (typically 6–10) grain

pairs from each meteorite show good reproducibility and trace elements appear to be homogeneous among clasts. Among all samples, light-middle REEs in opx are below detection limits but Dy, Y, Er and Yb have sufficient concentrations for accurate characterization. Light-heavy REEs in cpx are above detection limits and replicate analyses show good reproducibility. Our H chondrites show similar REE abundances and patterns to equilibrated LL chondrites (LL5-LL7) in cpx, but have lower abundances of heavy REEs in opx (Fig. 2).

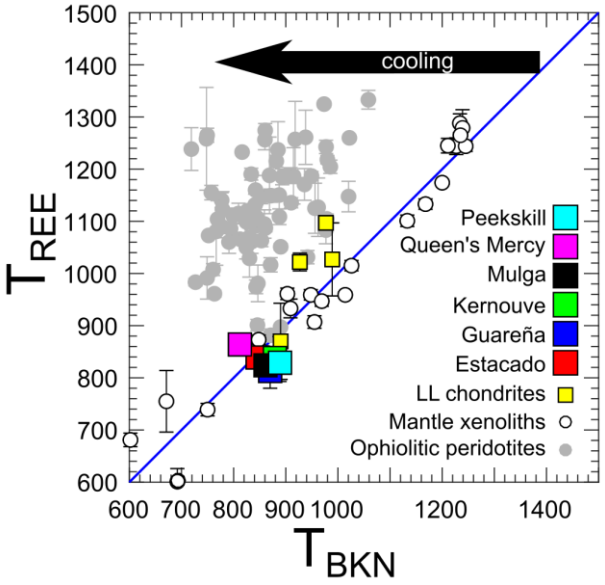

Figure 3. T_{REE} (y-axis) plotted against T_{BKN} (x-axis) (° C). H chondrites are large squares; also shown are four equilibrated LL chondrites [8], quenched mantle xenoliths from thermally stable environments [2], and ophiolitic peridotites that cooled slowly [3], which fall far to the left of the blue 1:1 line.

Temperatures: REE-in-two pyroxene temps (T_{REE}) are reported in Fig. 3 and the Table. T_{REE} (813-864°C) are in good agreement or slightly lower than temps (812-889°C) from the major element two-pyroxene thermometer of Brey and Köhler (T_{BKN}) [9]. T_{REE} uncertainties are obtained from scatter in the multi-element temperature inversion; sources of uncertainty may include failure to attain thermodynamic equilibrium during metamorphism, or discrepancies related to calibration. Ca-in-olivine ($T_{Ca\text{-}Ol}$) temps [10] are listed in the Table. $T_{Ca\text{-}Ol}$ (706-733°C) are in good agreement between the six samples. We consider Queen's Mercy temps as the least reliable as the sample exhibits shock effects (Shock Stage S2; see [11]), which may explain the observed major (Fig. 2) and trace element heterogeneity.

Discussion: At a temp of 850°C, REE lattice diffusion in opx is ~3 x 10^{-24} m^2/s [12], such that characteristic diffusion timescales for grain sizes relevant to the ordinary chondrites (~100 µm) are ~100 Myr. Thus, we infer that these T_{REE} are peak or near peak temps.

Sample	T_{REE}	2-Px[a]	T_{BKN}	ΔT	$T_{Ca\text{-}Ol}$
Estacado (H6)	839±18	-	846	-7	728
Guareña (H6)	813±33	848	870	-57	717
Kernouve (H6)	838±14	848	879	-41	712
Mulga North (H6)	824±1	-	861	-37	706
Peekskill (H6)	829±18	-	889	-60	712
Queen's M. (H6)	864±5	-	812	52	733

[a] Data from [7]; All temperatures given in ˚C

In contrast, T_{BKN} (based on the relatively rapid temp sensitive diffusive exchange of the diopside component between pyroxenes) often represent subsolidus cooling temps rather than peak temps. The difference between T_{REE} and T_{BKN} (ΔT) can be used to infer the cooling rate of a sample. Samples quenched from stable, high-temp environments (e.g., subcontinental mantle xenoliths; Fig. 3) have similar T_{REE} and T_{BKN}. Samples that cooled slowly (e.g., ophiolitic peridotites; Fig. 3) have higher T_{REE} than T_{BKN}. The agreement of T_{REE} and T_{BKN} among the H chondrites implies these samples were rapidly cooled from peak temps at >800°C. Simple closure temp models suggest the meteorites cooled through T_{BKN} and T_{REE} blocking temps at rates ≥1°C/year [13]. Similar models suggest that the meteorites cooled through $T_{Ca\text{-}Ol}$ blocking temps at ~10^{-3} °C/year. Such fast cooling is inconsistent with much slower rates inferred using techniques that record cooling rates at temps ≤500°C (e.g., metallography, fission tracks), which yield ~2-10°C/Myr rates for H chondrites [14,15]. Our results bolster the case for a thermal evolution that involves an early fragmentation-reassembly event [7], rather than *in situ* cooling at different depths in an onion-shell parent asteroid [6]. We hypothesize that the H chondrite parent body broke up at near-peak temps, quenching in similar T_{REE} and T_{BKN}. A challenge for the modeling community is to reconcile slow, low-temp cooling rates that are correlated with metamorphic grade (suggesting an onion-shell parent body [1,6]) with the fast rates we obtained for high-temp cooling intervals, which suggest catastrophic fragmentation of the H-chondrite parent body.

References: [1] McSween H.Y. et al. (2002) *Asteroids III, U.A. Press*, 559-571. [2] Liang Y., Sun C., Yao, L. (2013) *GCA*, 102, 246-260. [3] Dygert N., Liang, Y. (2015) *EPSL*, 420, 151–161. [4] Wang, C., Liang, Y., Xu, W. (2015) *Lithos*, 224-225, 101-113. [5] Liang, Y. et al. (2012) *LPSC XLIII*, #1987. [6] Harrison, K.P., Grimm, R.E. (2010) *GCA*, 74, 5410-5423. [7] Ganguly J. et al. (2013) *GCA*, 105, 206-220. [8] Dygert N. et al. (2018) *LPSC XLIX*, #1750. [9] Brey, G.P., Köhler, T. (1990) *J. Pet.*, 31(6), 1353-1378. [10] Köhler, T., Brey, G.P. (1990) *GCA*, 54, 2375-2388. [11] Rubin A.E. (2004) *GCA*, 68, 673-689. [12] Cherniak, D.Y., Liang, Y. (2007) *GCA*, 71, 1324-1340. [13] Dygert, N., Kelemen, P., Liang, Y. (2017) *EPSL*, 465, 134-144. [14] Taylor, G.J., et al. (1987) *Icarus, 69*, 1-13. [15] Trieloff et al. (2003) *Nature*, 422, 502-506.